

# TAbMEP Assessment: ICARTT j(O<sup>1</sup>D) Measurements

## 1. Introduction

Here we provide the assessment for the photolytic rate coefficient measurements of ozone photolysis to O<sup>1</sup>D, i.e. j(O<sup>1</sup>D). These measurements were taken from two aircraft platforms during the summer 2004 ICARTT field campaign [Fehsenfeld *et al.*, 2006, Singh *et al.*, 2006]. This assessment is based upon three wing-tip-to-wing-tip intercomparison flights conducted during the field campaign. Recommendations provided here offer TAbMEP assessed uncertainties for each of the measurements and a systematic approach to unifying the ICARTT j(O<sup>1</sup>D) data for any integrated analysis. These recommendations are directly derived from the instrument performance demonstrated during the ICARTT measurement comparison exercises and are not to be extrapolated beyond this campaign.

## 2. ICARTT j(O<sup>1</sup>D) Measurements

Two different j(O<sup>1</sup>D) instruments were deployed on two aircraft. Table 1 summarizes these techniques and gives references for more information.

**Table 1.** j(O<sup>1</sup>D) measurements deployed on aircraft during ICARTT

Aircraft	Instrument	Reference
NASA DC-8	Scanning Actinic Flux Spectroradiometers (SAFS)	<i>Shetter and Müller</i> [1999]
NOAA WP-3D	AFSR Actinic Flux Spectroradiometer (formerly: ZAPHROD)	<i>Stark et al.</i> [2007]

## 3. Summary of Results

Tables 2a and 2b summarize the assessed 2 $\sigma$  precisions, biases, and uncertainties. More detailed descriptions are provided to illustrate the process for assessment of bias and precision in Sections 4.1 and 4.2 respectively. The assessed 2 $\sigma$  precisions reported in Table 2 are equal to twice the highest adjusted precision value for that instrument listed in Table 4. Table 2 also reports an assessed bias (see Section 4.1 for details) that can be applied to maximize the consistency between the data sets. The assessed bias should be subtracted from the reported data to ‘unify’ the data sets. The assessed bias is derived from intercomparison periods only and may be extrapolated to the entire mission if one assumes instrument performance remained constant throughout the mission. The recommended 2 $\sigma$  uncertainty is the larger of either the uncertainty reported by the PI or the quadrature-sum of the assessed 2 $\sigma$  precision and assessed bias listed in Table 2. This analysis was split into two parts, j(O<sup>1</sup>D) values > 3x10<sup>-5</sup> (s<sup>-1</sup>) and j(O<sup>1</sup>D) values < 3x10<sup>-5</sup> (s<sup>-1</sup>), in order to achieve best results.

It should be noted here that photolysis rates of j(O<sup>1</sup>D) are not directly measurable. The photolysis rate,  $J$ , is calculated through a function of the compound’s absorption cross section  $\sigma(\lambda)$ , the quantum yield  $\Phi(\lambda)$ , and the actinic flux  $I(\lambda)$ :

$$J = \int_{\lambda_1}^{\lambda_2} \sigma(\lambda) \Phi(\lambda) I(\lambda) d\lambda \quad (1)$$

The actinic flux,  $I(\lambda)$ , is directly observed by the spectrometers onboard both aircraft; while the cross sections and quantum yields are measured in the laboratory. Thus, the uncertainties reported in Table 2 should be viewed as a weighted actinic flux measurement uncertainty over a

given range of the solar spectrum and solar zenith angles. In the case of ozone, the cutoff in the atmospheric spectra shifts to larger wavelength as zenith solar angle increases, which makes ozone absorption weaker and harder to measure, resulting in a larger uncertainty. Users requesting more information should contact Samuel Hall at [halls@ucar.edu](mailto:halls@ucar.edu) for DC-8 or Principal Investigator Harald Stark at [harald.stark@noaa.gov](mailto:harald.stark@noaa.gov) for WP-3D for detailed explanations.

**Table 2a.** Recommended ICARTT  $j(\text{O}^1\text{D})$  measurement treatment,  $j(\text{O}^1\text{D}) > 3 \times 10^{-5} (\text{s}^{-1})$

Aircraft/ Instrument	Reported Uncertainty <sup>a</sup>	Assessed 2 $\sigma$ Precision	Assessed Bias ( $\text{s}^{-1}$ )	Assessed 2 $\sigma$ Uncertainty
NASA DC-8 SAFS	12.3%	1.0%	$0.00 + 0.02 j(\text{O}^1\text{D})_{\text{DC8}}$	Quadrature Sum
NOAA WP-3D AFSR	30%	5.2%	$0.00 - 0.04 j(\text{O}^1\text{D})_{\text{WP3D}}$	30% <sup>b</sup>

<sup>a</sup>User should see text or consult Samuel Hall at [halls@ucar.edu](mailto:halls@ucar.edu) for DC-8 or PI Harald Stark at [harald.stark@noaa.gov](mailto:harald.stark@noaa.gov) for WP-3D prior to utilizing this data for explanation of uncertainty values.

<sup>b</sup>This recommendation based on test ranging from  $3 \times 10^{-5}$  to  $7 \times 10^{-5} j(\text{O}^1\text{D}) (\text{s}^{-1})$ .

**Table 2b.** Recommended ICARTT  $j(\text{O}^1\text{D})$  measurement treatment,  $j(\text{O}^1\text{D}) < 3 \times 10^{-5} (\text{s}^{-1})$

Aircraft/ Instrument	Reported Uncertainty <sup>a</sup>	Assessed 2 $\sigma$ Precision	Assessed Bias ( $\text{s}^{-1}$ )	Assessed 2 $\sigma$ Uncertainty
NASA DC-8 SAFS	12.3%	1.4%	$0.00 - 0.07 j(\text{O}^1\text{D})_{\text{DC8}}$	Quadrature Sum
NOAA WP-3D AFSR	30%	53%	$0.00 + 0.17 j(\text{O}^1\text{D})_{\text{WP3D}}$	Quadrature Sum <sup>b</sup>

<sup>a</sup>User should see text or consult Samuel Hall at [halls@ucar.edu](mailto:halls@ucar.edu) for DC-8 or PI Harald Stark at [harald.stark@noaa.gov](mailto:harald.stark@noaa.gov) for WP-3D prior to utilizing this data for explanation of uncertainty values.

<sup>b</sup>This recommendation based on test ranging from  $1 \times 10^{-6}$  to  $2.9 \times 10^{-5} j(\text{O}^1\text{D}) (\text{s}^{-1})$ .

Figures 1a-1c and 2a-2c display the precisions, biases, and recommended uncertainties for the two  $j(\text{O}^1\text{D})$  instruments that measured values above  $3 \times 10^{-5} (\text{s}^{-1})$  and below  $3 \times 10^{-5} (\text{s}^{-1})$ , respectively. In both cases, the uncertainty is driven by precision.

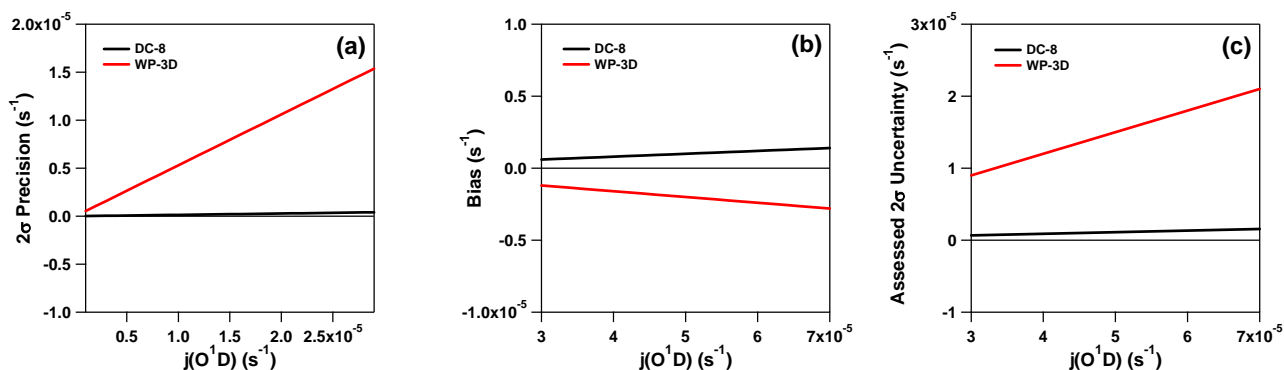


**Figure 1.**  $2\sigma$  precision (panel a), bias (panel b), and assessed  $2\sigma$  uncertainty (panel c) for DC-8 (black) and WP-3D (red) as a function of  $j(\text{O}^1\text{D})$  level. Values were calculated based upon data shown in Table 2a for  $j(\text{O}^1\text{D})$  values greater than  $3 \times 10^{-5} (\text{s}^{-1})$ .

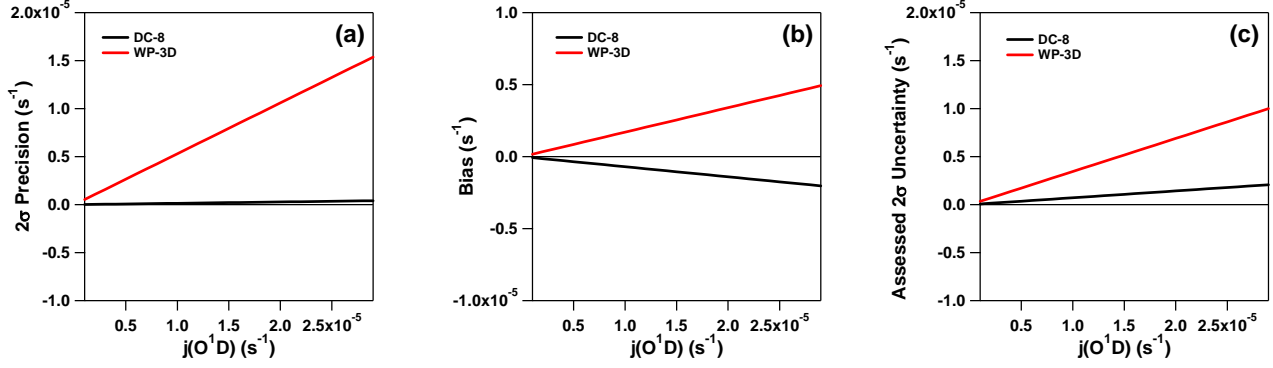


**Figure 2.**  $2\sigma$  precision (panel a), bias (panel b), and assessed  $2\sigma$  uncertainty (panel c) for DC-8 (black) and WP-3D (red) as a function of  $j(O^1D)$  level. Values were calculated based upon data shown in Table 2b for  $j(O^1D)$  values less than  $3 \times 10^{-5} (s^{-1})$ .

## 4. Results and Discussion

### 4.1 Bias Analysis

Section 3.3 in the introduction describes the process used to determine the best estimate bias. The linear relationships listed in Table 3a were derived from the regression equation found in Figure 3 (07/22/2004 correlation) as this was the only date with  $j(O^1D)$  values greater than  $3 \times 10^{-5}$ . Linear relationships listed in Table 3b were derived from the regression equation found in Figure 4 for  $j(O^1D)$  values less than  $3 \times 10^{-5}$ . It should be noted that the regression lines were forced to zero in all cases. The reference standard for comparison (RSC) is constructed by averaging weighted values of NOAA WP-3D and NASA DC-8. Weighted values shown in Equation 2 were used to best resolve technical difficulties that were experienced by the WP-3D AFSR instrument during the series of flights.

$$RSC = \begin{cases} \frac{2 SAES_3 + AFSR}{3} jO^1D > 3 \times 10^{-5} \\ \frac{3 SAES_4 + AFSR}{4} jO^1D < 3 \times 10^{-5} \end{cases} \quad (2)$$

The resulting RSC's can be expressed as a function of the DC-8  $j(O^1D)$  measurement as the following:

$$RSC_{jO1D} = 0.00 + 0.98 j(O^1D)_{DC8}; j(O^1D) \text{ values} > 3 \times 10^{-5} (s^{-1}) \quad (3)$$

$$RSC_{jO1D} = 0.00 + 1.07 j(O^1D)_{DC8}; j(O^1D) \text{ values} < 3 \times 10^{-5} (s^{-1}) \quad (4)$$

The RSC is then used to calculate the best estimate bias as described in Section 3.3 of the introduction. It should be noted that the initial choice of the reference instrument (DC-8 SAFS) is arbitrary, and has no impact on the final recommendations. Tables 3a and 3b summarize the assessed measurement bias for each of the two ICARTT  $j(O^1D)$  measurements.

**Table 3a.** ICARTT  $j(O^1D)$  bias estimates,  $j(O^1D) > 3 \times 10^{-5} (s^{-1})$ 

Aircraft/ Instrument	Linear Relationships <sup>a</sup>	Best Estimate Bias ( $a + b j(O^1D)$ ) ( $s^{-1}$ )
NASA DC-8 SAFS	$0.00 + 1.00 j(O^1D)_{DC8}$	$0.00 + 0.02 j(O^1D)_{DC8}$
NOAA WP-3D ZAPHROD	$0.00 + 0.94 j(O^1D)_{DC8}$	$0.00 - 0.04 j(O^1D)_{WP3D}$

<sup>a</sup>Derived from Fig. 3 (7/22 correlation).

**Table 3b.** ICARTT  $j(O^1D)$  bias estimates,  $j(O^1D) < 3 \times 10^{-5} (s^{-1})$ 

Aircraft/ Instrument	Linear Relationships <sup>a</sup>	Best Estimate Bias ( $a + b j(O^1D)$ ) ( $s^{-1}$ )
NASA DC-8 SAFS	$0.00 + 1.00 j(O^1D)_{DC8}$	$0.00 - 0.07 j(O^1D)_{DC8}$
NOAA WP-3D ZAPHROD	$0.00 + 1.29 j(O^1D)_{DC8}$	$0.00 + 0.17 j(O^1D)_{WP3D}$

<sup>a</sup>Derived from Fig. 4.

#### 4.2 Precision Analysis

A detailed description of the precision assessment is given in Section 3.1 of the introduction. The IEIP precision, expected variability, observed variability, and the adjusted precision are summarized in Table 4. Dissimilar to other TAbMEB assessment reports, the precision and variability are reported based upon the ranges of  $j(O^1D)$  values instead of dates of intercomparison flights. It should be noted that flight dates and  $j$ -values do correspond with one another-  $j(O^1D)$  values greater than  $10^{-5}$  were reported on 7/22/2004,  $j(O^1D)$  values below  $10^{-6}$  were reported on 7/31/2004, and  $j(O^1D)$  values between  $10^{-6}$  and  $10^{-5}$  were reported on 8/07/2004. Based on the results presented in Table 4, the largest "adjusted precision" value is taken as a conservative precision estimate for each ICARTT  $j(O^1D)$  instrument and twice that value is listed in Tables 2a and 2b as the assessed  $2\sigma$  precision.

To minimize the effect of bias, we make corrections for bias before computing the observed variability, as the bias may have a significant impact on the observed variability. Figure 6 shows the magnitude of the bias for each intercomparison. The assessed values of the observed variability are displayed in Figure 7. The final analysis results are shown in Tables 2a and 2b.

**Table 4.** ICARTT  $j(O^1D)$  precision ( $1\sigma$ ) comparisons

$j(O^1D)$ Range	Platform	IEIP Precision	Expected Variability	Observed Variability	Adjusted Precision
$>10^{-5}$ (7/22)	DC-8	0.3%	1.5%	2.6%	0.5%
	WP-3D	1.5%			2.6%
$<10^{-6}$ (7/31)	DC-8	0.2%	7.5%	26.5%	0.7%
	WP-3D	7.5%			26.5%
$10^{-6} - 10^{-5}$ (8/07)	DC-8	0.3%	4.5%	7.0%	0.5%
	WP-3D	4.5%			7.0%

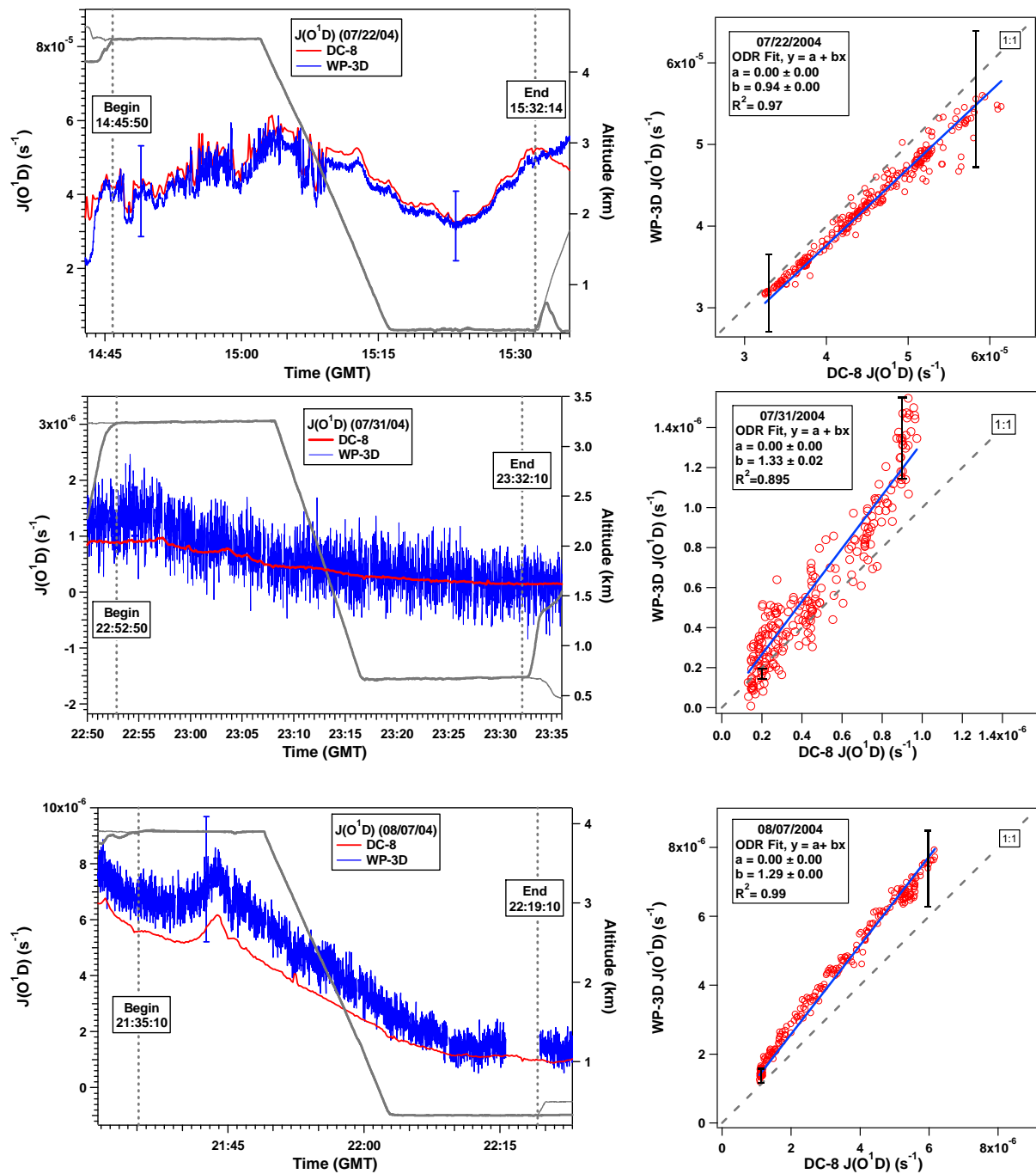


**Figure 3.** (left panels) Time series of  $j(\text{O}^1\text{D})$  measurements and aircraft altitudes from two aircraft on the three intercomparison flights between the NASA DC-8 and the NOAA WP-3D. (right panels) Correlations between the  $j(\text{O}^1\text{D})$  measurements on the two aircraft. Error bars shown depict the reported measurement uncertainties.

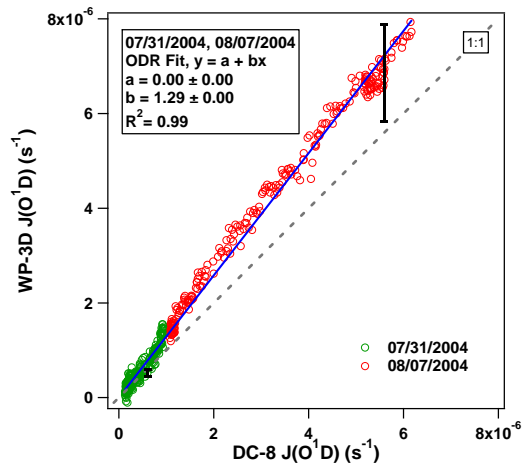


**Figure 4.** Correlation between the  $j(O^1D)$  measurements on the DC-8 and WP-3D for 7/31 and 8/07 2004. Error bars shown depict the reported measurement uncertainties.

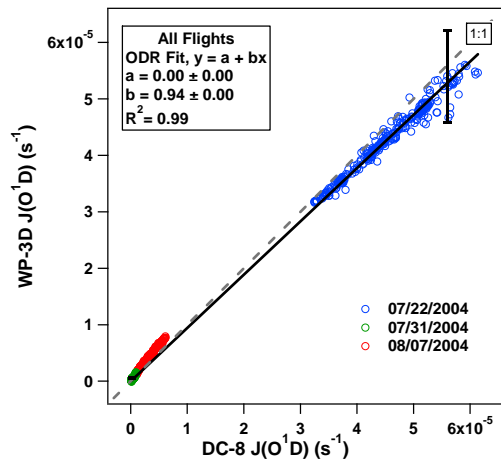


**Figure 5.** Correlation between the  $j(O^1D)$  measurements on the DC-8 and WP-3D for 7/22, 7/31, and 8/7 2004. Error bars shown depict the reported measurement uncertainties.

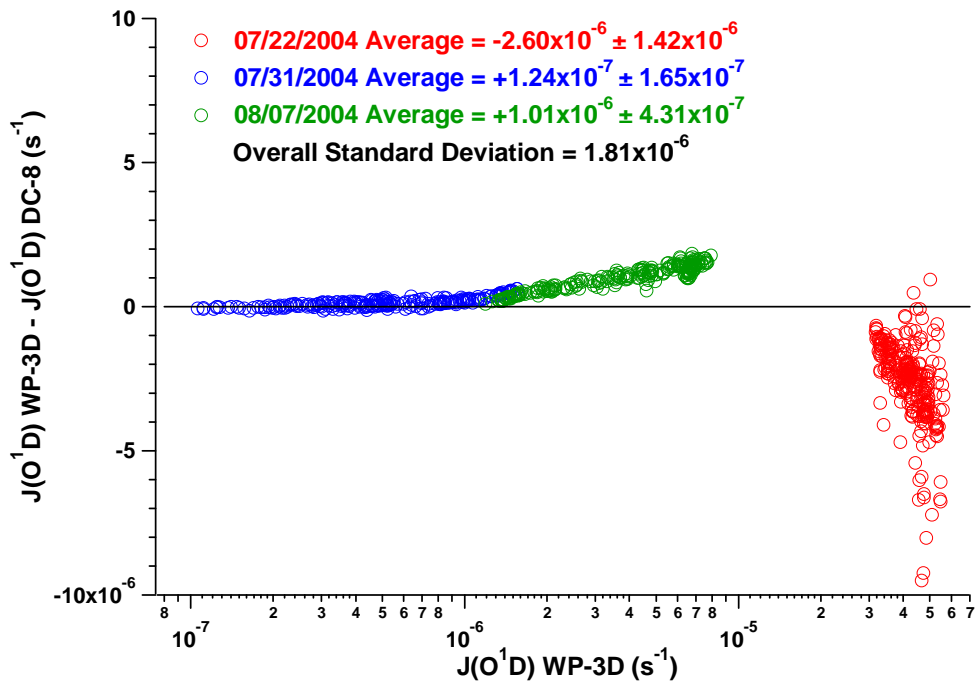


**Figure 6.** Difference between  $j(O^1D)$  measurements from the three DC-8/WP-3D intercomparison flights as a function of the WP-3D  $j(O^1D)$ .

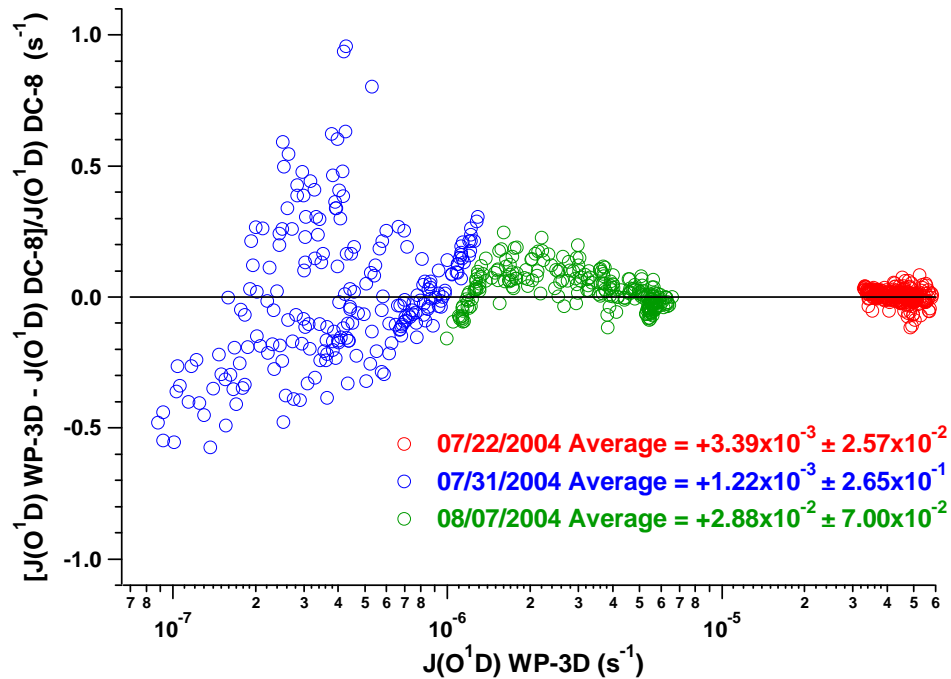


**Figure 7.** Relative difference between  $j(O^1D)$  measurements from the three DC-8/WP-3D intercomparison flights as a function of the WP-3D  $j(O^1D)$ . A correction was made to account for bias.

## References

- Fehsenfeld, F. C., et al. (2006), International Consortium for Atmospheric Research on Transport and Transformation (ICARTT): North America to Europe—Overview of the 2004 summer field study, *J. Geophys. Res.*, *111*, D23S01, doi:10.1029/2006JD007829.
- Shetter, R. E. and M. Müller (1999), Photolysis frequency measurements on the NASA DC-8 during the PEM-Tropics Mission using actinic flux spectroradiometry: Instrumentation description and results, *J. Geophys. Res.*, *104*, 5647-5661.
- Singh, H. B., et al. (2006), Overview of the summer 2004 Intercontinental Chemical Transport Experiment-North America (INTEX-A), *J. Geophys. Res.*, *111*, D24S01, doi:10.1029/2006JD007905.
- Stark, H., et al. (2007), Atmospheric in-Situ Measurement of Nitrate Radical (NO<sub>3</sub>) and Other Photolysis Rates Using Spectro- and Filter Radiometry, *J. Geophys. Res.*, *112*, D10S04, doi:10.1029/2006JD007578.